Supporting Information

Surfactant modified Zn nanosheets on carbon paper for electrochemical CO_2 reduction to CO

Wenyuan Wang,[a] Xuhua He,[a] Kai Zhang,[a] Yagang Yao[a,*]

[a] National Laboratory of Solid State Microstructures, College of Engineering and Applied Sciences, Jiangsu Key Laboratory of Artificial Functional Materials, and Collaborative Innovation Center of Advanced Microstructures, Nanjing University, Nanjing 210093, China

E-mail: ygyao2018@nju.edu.cn

EXPERIMENTAL SECTION

Chemical Reagents

NaOH (electronic grade), $Zn(NO_3)_2 \cdot 6H_2O$ (AR), $Na_3C_6H_5O_7 \cdot 2H_2O$ (AR), isopropyl alcohol (C_3H_8O, AR), potassium bicarbonate ($KHCO_3$, AR) and hexadecyl trimethyl ammonium bromide (CTAB, $C_{19}H_{42}BrN$, 99 %) were all purchased from Aladdin Industrial Corporation. Nafion solution (D-521, 5 wt %) was purchased from Alfa Aesar. Acetone (C_3H_6O, AR) and ethanol (C_2H_5OH, AR) were bought from Sinopharm. We didn't further purify the whole reagents used in the experiment.

Synthesis of 3D flower-like ZnO nanoplates (ZnO NFs)

Zinc nitrate hexahydrate (8.88 g) and sodium citrate dehydrate (21.12 g) were dissolved in 300 mL ultra-pure water (18.25 MΩ). Then, 100 mL sodium hydroxide solution (60 mg mL^{-1}) was gradually poured into the zinc nitrate solution. The mixed solution was stirred under magnetic force at room temperature for two hours. Vacuum suction filtration was employed to separate the 3D flower-like ZnO NFs from the solution. The sample was continued to be rinsed for three times after the water was drained. The obtained samples were dried using drying box under 50 °C for 12 hours.

Characterizations

XRD was used to confirm the sample phase on LabX-6000 of Shimadzu with the emission wavelength of 1.54 Å via Cu Kα radiation, and the sweep velocity is 5° min^{-1}. SEM was performed to take the picture of sample microdomains on SU8100 from Hitachi, and the operating voltage is 5 KV. The sample structure was determined via TEM on TF20 of FEI with the operating potential of 200 kV. XPS was employed to analyze the element information in samples on Thermo ESCALAB 250XI with the energy of 1486.7 eV through Al Kα radiation.

The functional group of CTAB was confirmed through FT-IR on Nicolet iS10, which is equipped with an ATR detector. Zeta potential measurement was carried out to characterize the charge distribution of Zn NFs modified with various amount of CTAB (0, 0.05, 0.8, 1.6, 3.2 mg) on Malvern Nano-Z.

Preparation of working electrode

The carbon paper (TGP-H-060, Toray) was ultrasonicated in acetone, ethanol and ultra-pure water for 30 minutes. The moisture of pretreated carbon paper was removed by drying oven under 50 °C for 24 hours. Ten milligrams 3D flower-like ZnO nanoplates were mixed with one milliliter isopropyl alcohol and twenty microliters Nafion solution (5 wt %). The mixed solution was sonicated for half hour. Forty microliters catalyst solution was transferred on carbon paper with a pipette gun, followed by drying in the natural environment overnight. The effective area of electrode is 1 cm^{-2}. The zinc NFs was fabricated through *in situ* electrochemical reduction from ZnO NFs in 0.5 M potassium bicarbonate solution under -1.0 V for half hour with argon atmosphere. CTAB was dissolved into isopropyl alcohol to prepare the solution. Forty microliters of CTAB solution (1.25 mg mL^{-1}) was dropped onto the Zn NFs electrode to obtain Zn NFs-0.05. Forty microliters of CTAB solution (20 mg mL^{-1}) was dropped onto the Zn NFs electrode to obtain Zn NFs-0.8. A total of 80 μL of CTAB solution (20 mg mL^{-1}) was dropped onto the Zn NFs electrode to obtain Zn NFs-1.6. A total of 160 μL of CTAB solution (20 mg mL^{-1}) was dropped onto the Zn NFs electrode to obtain Zn NFs-3.2. Then, all the CTAB-modified Zn NFs electrode were dried under an infrared baking lamp for 30 min.

Electrochemical measurement

The H-cell (Gaoss Union) device was employed to conduct electrochemical measurement on electrochemical workstation (CHI760E). The DuPont Nafion®117 was used as the proton exchange membrane. Each chamber was pured into thirty milliliters potassium bicarbonate solution solution (0.5 M). Ag/AgCl and platinum foil electrode (2 × 2 cm) were used in the experiment. The dissolved oxygen in aqueous solution was previously removed through pumping in carbon dioxide (99.999 %) for half hour. The applied potentials were converted by the subsequent formula: $E_{RHE} = E_{Ag/AgCl} + 0.197\ V + 0.05916 \times pH$, while the pH value is equal to 7.2.[1] LSV was recorded from 0 to -1.1 V, and the test speed is 10 mV per minute. The electrochemical active surface area (ECSA) was calculated as follows: ECSA = $(C_{dl} / C_s) \times S$.[2] C_{dl} is double layer capacitance, which is estimated through fitting ampere density difference and test speed under -0.05 V. C_s is the double layer capacitance per unit area of smooth sample in identical electrolyte conditions (C_s = 30 μF cm^{-2}).[3] S is the geometric area of working electrode (S = 1 cm^2, in this work). The EIS plots were evaluated in potassium bicarbonate solution solution (0.5 M) from 100000 to 0.1 hertz under -0.7 V. The Tafel slope is calculated as follows: taking the overpotential as the Y-axis coordinate and the logarithm of the negative value of the CO partial current density (j_{CO}) as the X-axis coordinate. The slope obtained by fitting the linear part is the Tafel slope. Single oxidative LSV data was measured in potassium hydroxide solution (0.1 M).

Product analysis

The gas chromatography (GC9860) was used to constantly count CO and H_2. The analysis instrument is outfitted with TCD and FID with methanizer. The FE of hydrogen and carbon monoxide was calculated by the subsequent formula:

$$FE = \frac{c \times m \times nFP}{RTI_{total}} \times 100\%$$

where c stands for the concentration of CO and H_2, m is the CO_2 mass flow, n is equal to two for hydrogen or carbon monoxide, F is equal to 96485 C mol^{-1}, P is equal to 101325 Pa, R is equal to 8.314 J mol^{-1} K^{-1}, T is the ambient temperature, and I_{total} is the current obtained from the electrochemical workstation.[4]

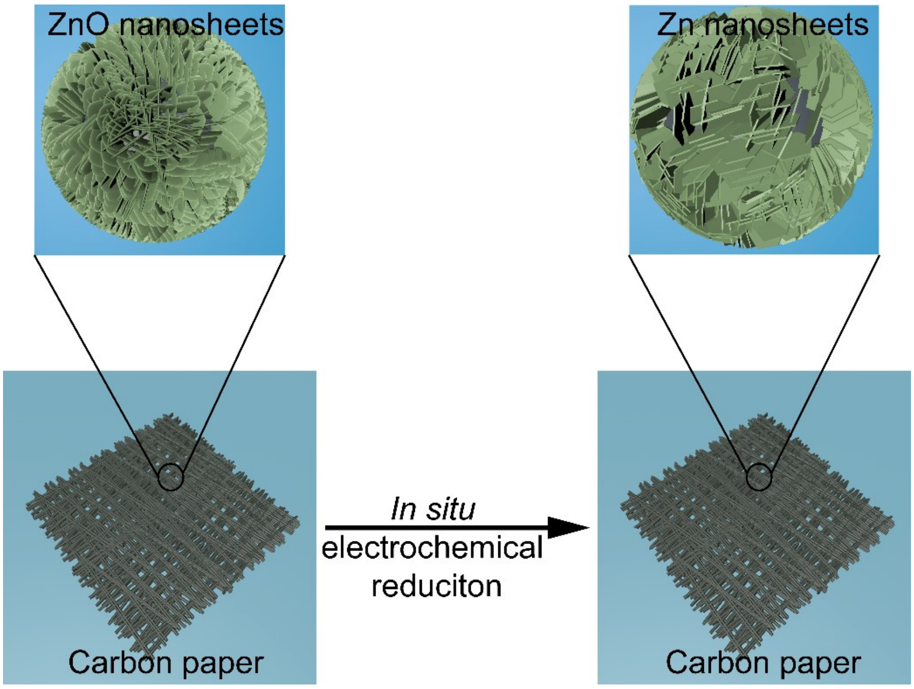

Scheme S1. The schematic of *in situ* electrochemical reduction of ZnO nanosheets to Zn nanosheets on carbon paper in 0.5 M $KHCO_3$ under -1.0 V for half hour with argon atmosphere.

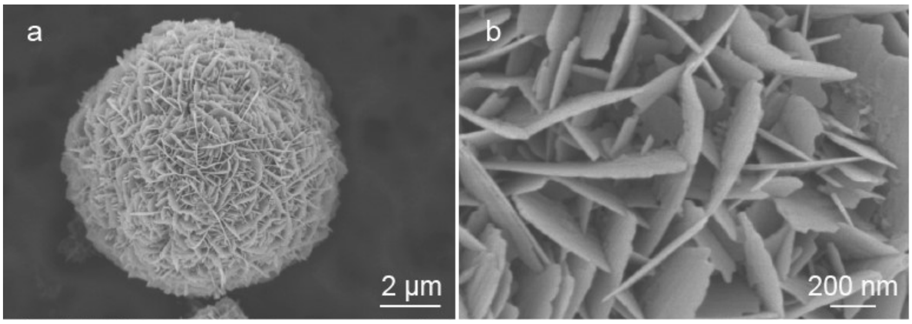

Figure S1. (a, b) SEM images of ZnO NFs.

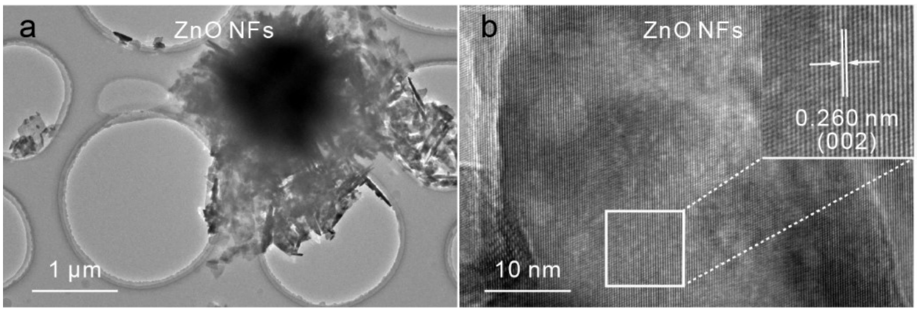

Figure S2. (a) TEM image of ZnO NFs. (b) HRTEM image of ZnO NFs.

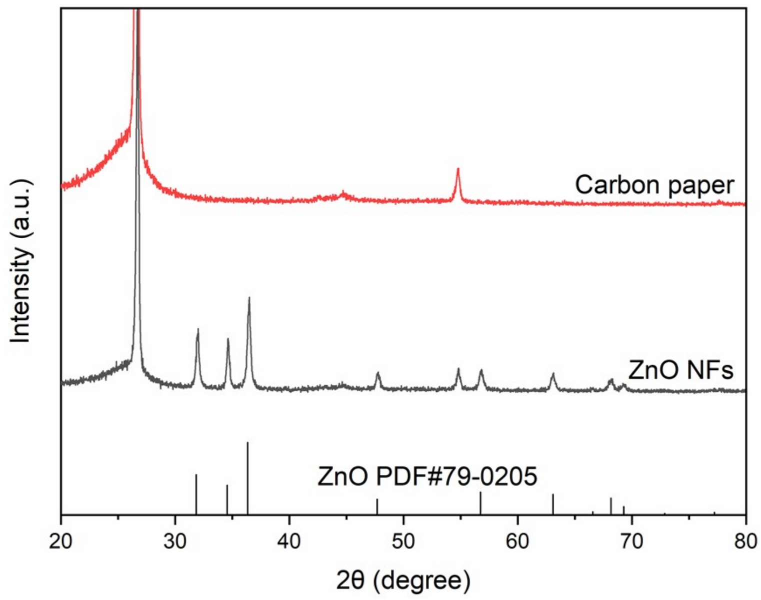

Figure S3. XRD patterns of carbon paper and ZnO NFs.

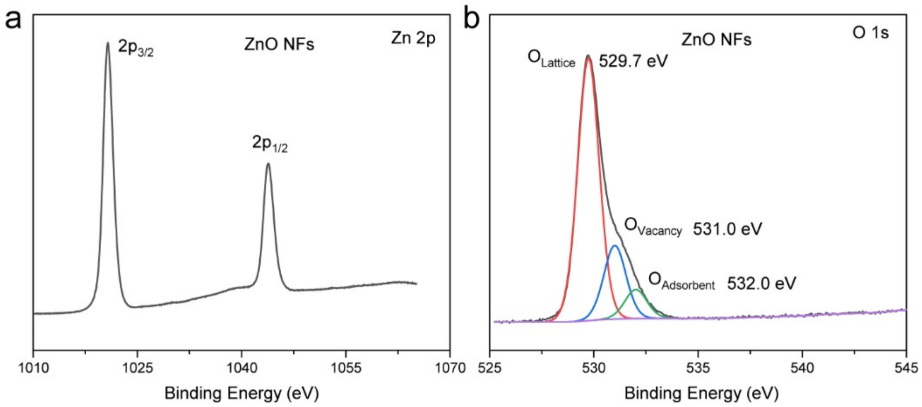

Figure S4. (a) Zn 2p XPS spectra of ZnO NFs. (b) O 1s XPS spectra of ZnO NFs.

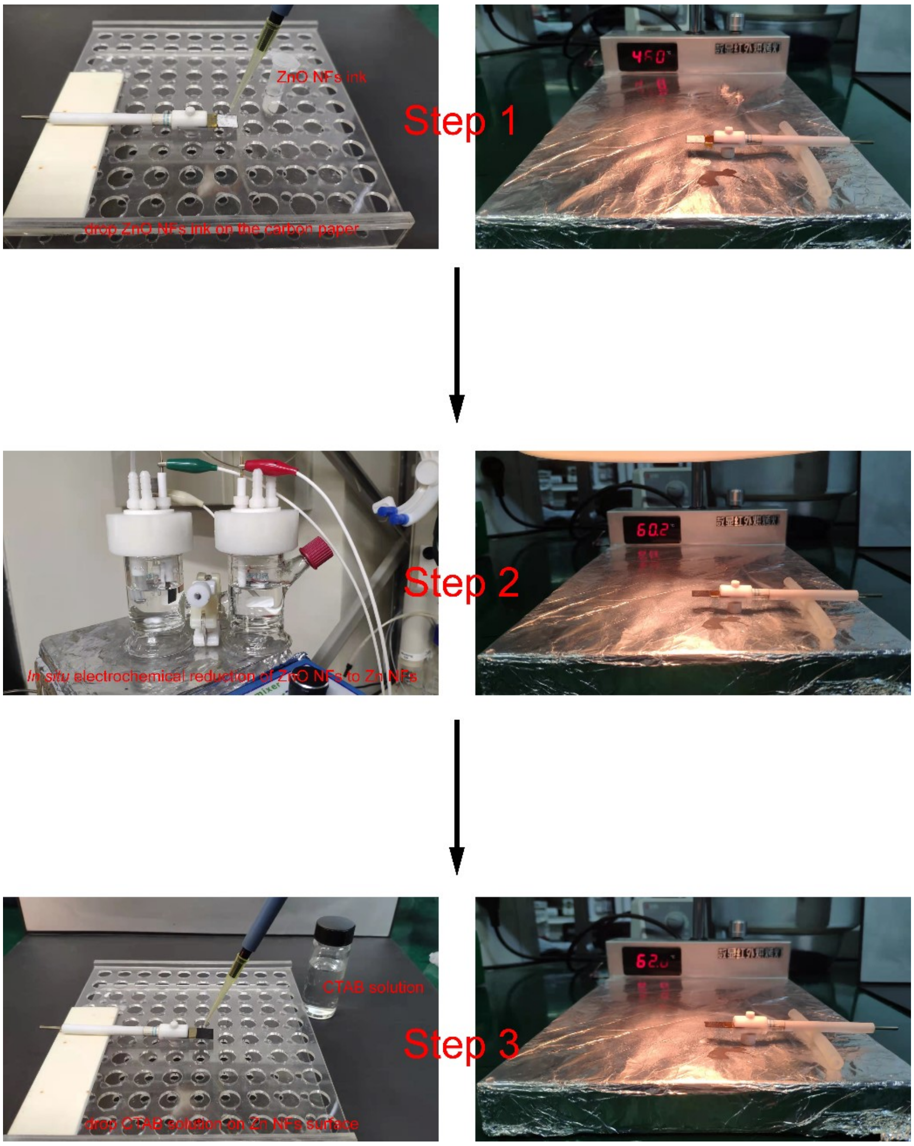

Figure S5 The schematic of the electrode preparation in detail.

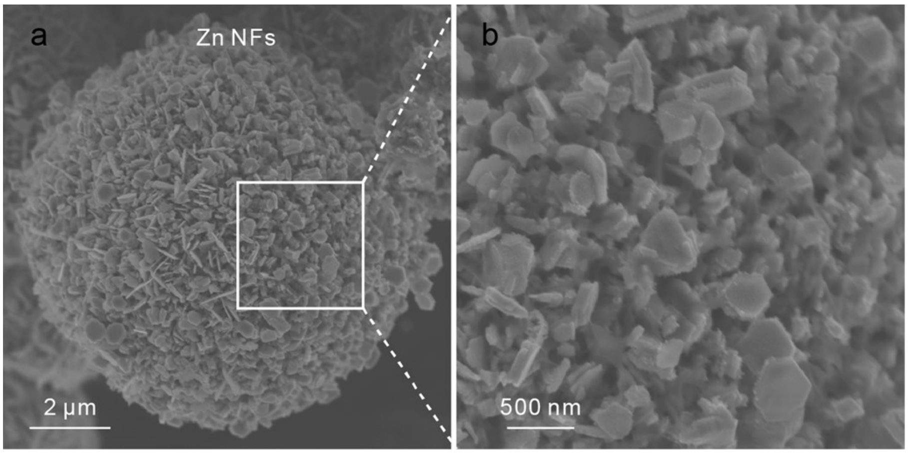

Figure S6. (a, b) SEM images of Zn NFs.

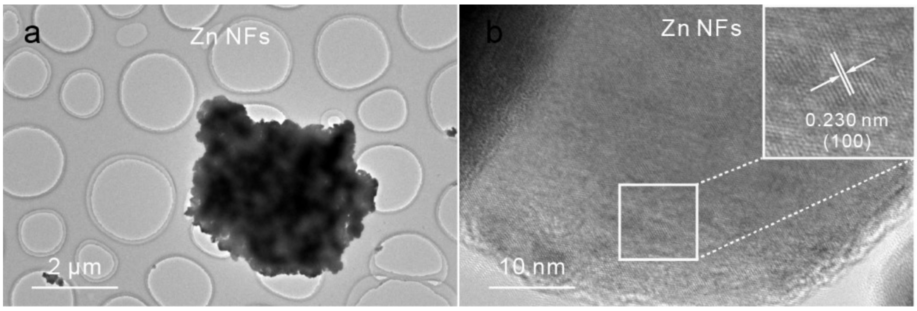

Figure S7. (a, b) TEM and HRTEM images of Zn NFs.

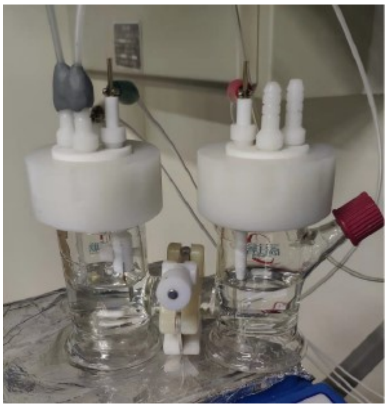

Figure S8. Schematic of H-type cells for electrochemical CO_2 reduction.

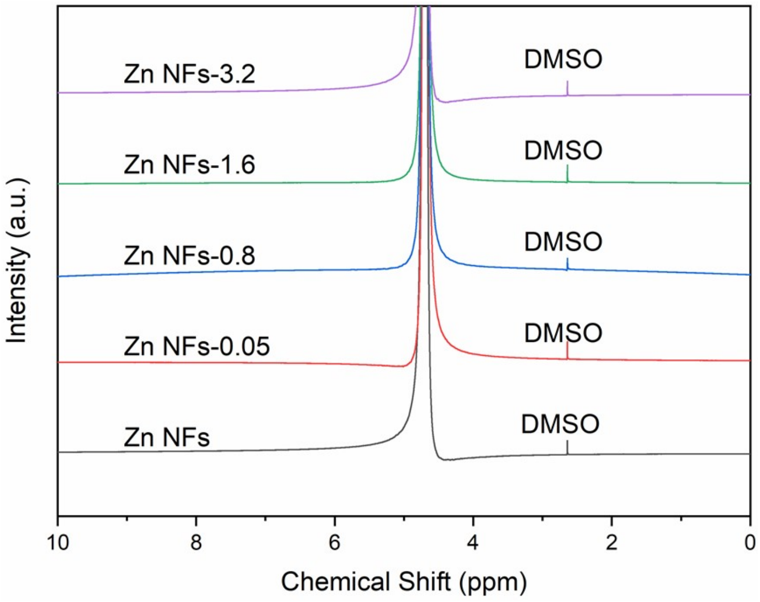

Figure S9. NMR spectrum of the post-electrolysis solution. The the post-electrolysis solution was analyzed on 400 MHz Bruker Advance**.** The liquid sample consisted of 300 μL catholyte, 200 μL D_2O and 100 μL DMSO (1/1000, v/v). The scan number was 64.

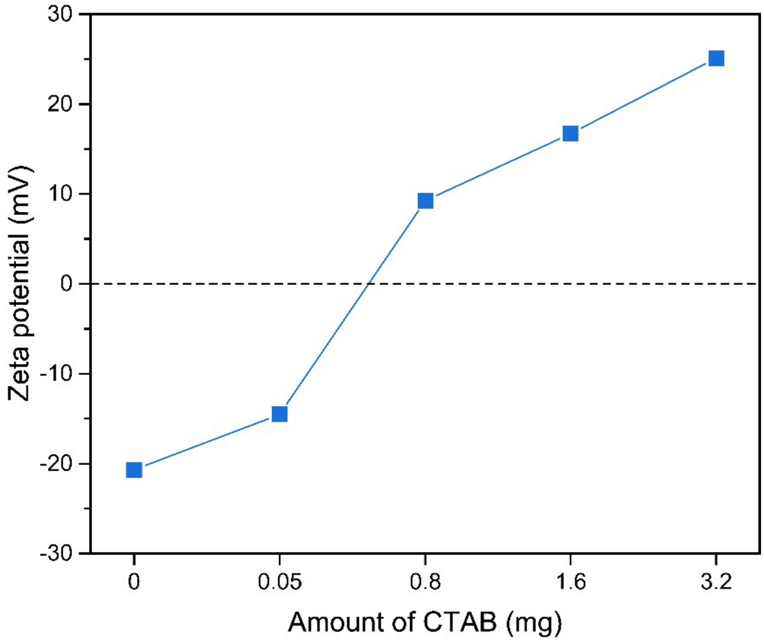

Figure S10. Zeta potentials of Zn NFs with various amount of CTAB (0, 0.05, 0.8, 1.6, 3.2 mg) in 0.5 M $KHCO_3$ electrolyte.

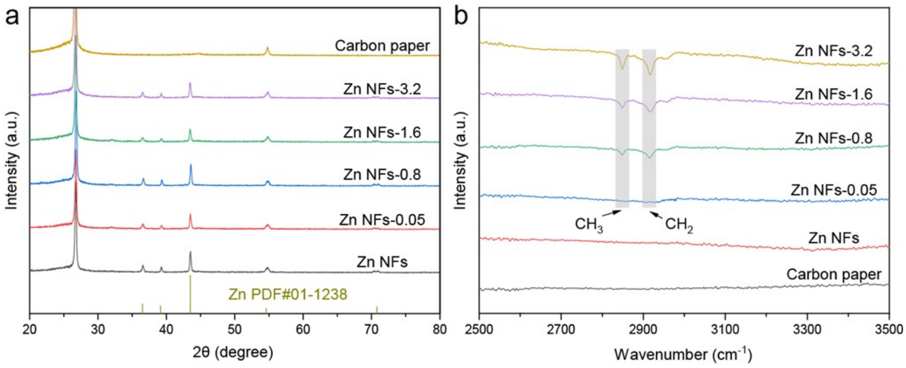

Figure S11. (a) XRD patterns of as-prepared samples after CO_2RR. (b) FT-IR spectroscopy of as-prepared samples after CO_2RR.

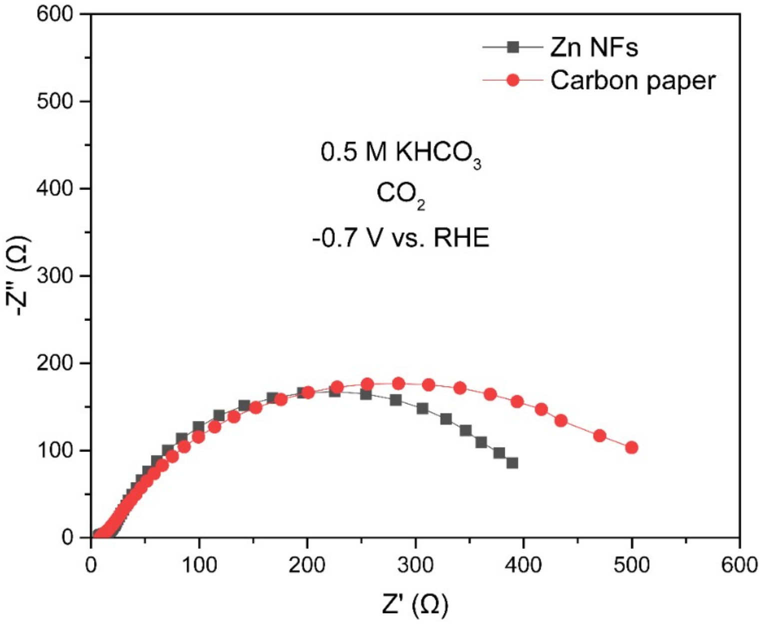

Figure S12. The EIS curves of Zn NFs and carbon paper.

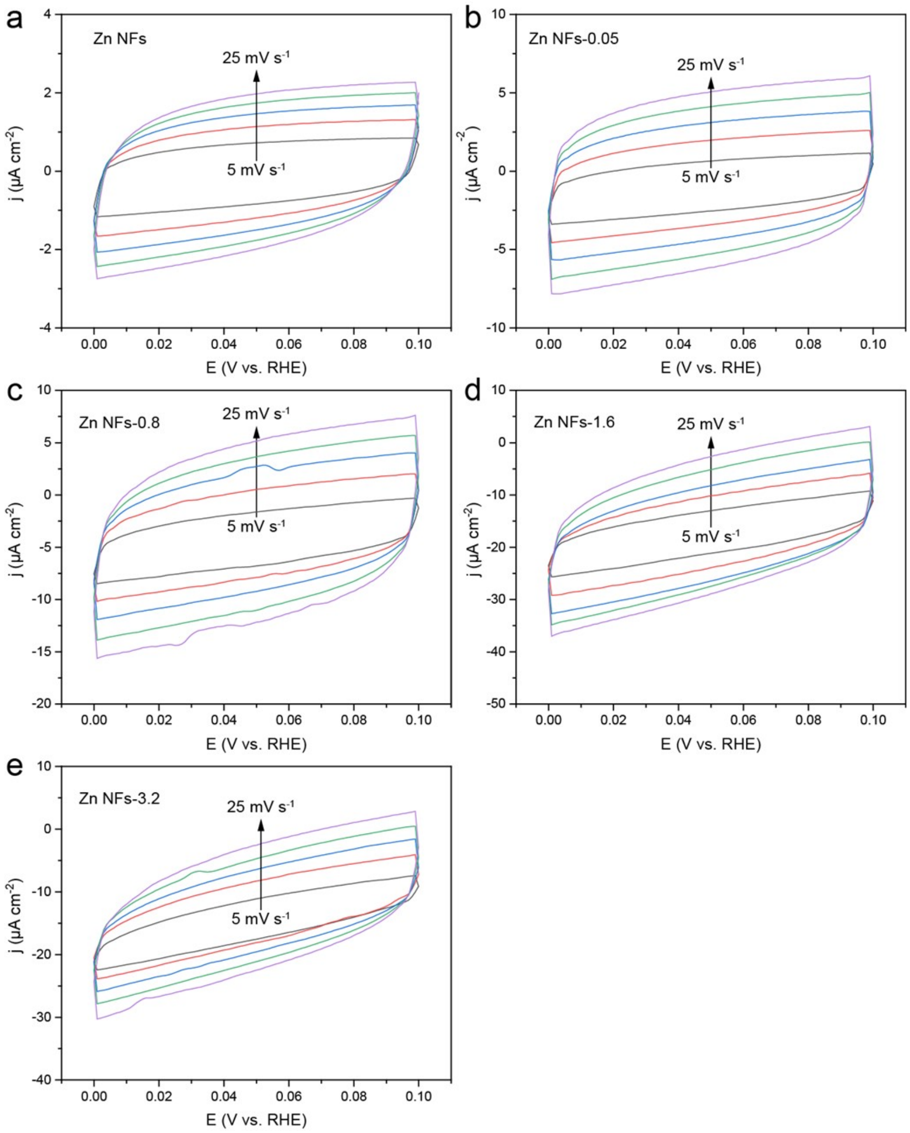

Figure S13. CV curves of Zn NFs modified with different amount CTAB (0, 0.05, 0.8, 1.6, and 3.2 mg) at different scan rate (5, 10, 15, 20 and 25 mV s^{-1}).

2θ	(hkl)
31.8°	(100)
34.5°	(002)
36.3°	(101)
47.6°	(102)
56.7°	(110)
63.0°	(103)
66.5°	(200)
68.0°	(112)
69.2°	(201)
72.6°	(004)
77.2°	(202)

Table S1. The individual XRD peaks of ZnO NFs (PDF # 79-0205).

Electrode	FE_{CO} (%)					
	-0.6 V	-0.7 V	-0.8 V	-0.9 V	-1.0 V	-1.1 V
Zn NFs	15.3	20.2	37.9	55.5	66.3	70.8
Zn NFs-0.05	21.5	37.4	55	71.2	80.4	84.1
Zn NFs-0.8	50.4	66.2	79.3	84.5	87.9	90
Zn NFs-1.6	62.4	72.3	86.3	91.1	94.2	95.6
Zn NFs-3.2	54.3	69.9	83.9	88.7	90.6	91.7

Table S2. CO Faraday efficiency (FE_{CO}) of Zn NFs modified with various amount of CTAB (0, 0.05, 0.8, 1.6, 3.2 mg) at different applied voltages.

Electrode	Electrolyte	E vs. RHE (V)	FE_{CO} (%)	J_{CO} (mA cm^{-2})	Reference
Ni SAs/N-C	0.5 M $KHCO_3$	-1.00	72.0	10.5	5
PD-Zn/Ag	0.1 M $KHCO_3$	-1.24	73.3	9.5	6
RE-Zn-CO_2	0.5 M $KHCO_3$	-1.00	77.6	8.4	7
Zn dendrite	0.5 M $NaHCO_3$	-1.10	79.0	13.4	8
V_o-rich ZnO	0.1 M $KHCO_3$	-1.10	83.0	16.1	9
h-Zn	0.5 M $KHCO_3$	-0.95	85.4	9.5	10
MZnNSs	0.5 M $NaHCO_3$ and 0.1 M H_2SO_4	-1.13	86.0	5.2	11
$Zn_{94}Cu_6$	0.5 M $KHCO_3$	-0.95	90.0	7.1	12
Zn P-NS	0.1 M $KHCO_3$	-1.00	90.0	7.4	13
LiET-Zn	0.1 M $KHCO_3$	-1.17	91.1	23	14
Zn NFs-1.6	0.5 M $KHCO_3$	-1.10	95.6	12.5	This work

Table S3. FE_{CO} and current density of electrochemical CO_2 reduction to CO reported in reference.

Electrode	ECSA/cm^2
Zn NFs	4
Zn NFs-0.05	13.4
Zn NFs-0.8	20.4
Zn NFs-1.6	30
Zn NFs-3.2	22.5

Table S4. Electrochemical active surface area (ECSA) of each electrode.

Reference

1. X. Wang, Z. Chen, X. Zhao, T. Yao, W. Chen, R. You, C. Zhao, G. Wu, J. Wang, W. Huang, J. Yang, X. Hong, S. Wei, Y. Wu and Y. Li, *Angew. Chem. Int. Edit.*, 2018, **57**, 1944-1948.
2. C. C. L. McCrory, S. Jung, J. C. Peters and T. F. Jaramillo, *J. Am. Chem. Soc.*, 2013, **135**, 16977-16987.
3. K. Ye, Z. Zhou, J. Shao, L. Lin, D. Gao, N. Ta, R. Si, G. Wang and X. Bao, *Angew. Chem. Int. Edit.*, 2020, **59**, 4814-4821.
4. Y. Wang, C. Niu, Y. Zhu, D. He and W. Huang, *ACS Applied Energy Materials*, 2020, **3**, 9841-9847.
5. C. Zhao, X. Dai, T. Yao, W. Chen, X. Wang, J. Wang, J. Yang, S. Wei, Y. Wu and Y. Li, *J. Am. Chem. Soc.*, 2017, **139**, 8078-8081.
6. Q. H. Low, N. W. X. Loo, F. Calle-Vallejo and B. S. Yeo, *Angew. Chem. Int. Edit.*, 2019, **58**, 2256-2260.
7. D. L. T. Nguyen, M. S. Jee, D. H. Won, H. Jung, H.-S. Oh, B. K. Min and Y. J. Hwang, *ACS Sustain. Chem. Eng.*, 2017, **5**, 11377-11386.
8. J. Rosen, G. S. Hutchings, Q. Lu, R. V. Forest, A. Moore and F. Jiao, *ACS Catal.*, 2015, **5**, 4586-4591.
9. Z. Geng, X. Kong, W. Chen, H. Su, Y. Liu, F. Cai, G. Wang and J. Zeng, *Angew. Chem. Int. Edit.*, 2018, **57**, 6054-6059.
10. D. H. Won, H. Shin, J. Koh, J. Chung, H. S. Lee, H. Kim and S. I. Woo, *Angew. Chem. Int. Edit.*, 2016, **55**, 9297-9300.
11. T. Zhang, X. Li, Y. Qiu, P. Su, W. Xu, H. Zhong and H. Zhang, *J. Catal.*, 2018, **357**, 154-162.
12. P. Moreno-García, N. Schlegel, A. Zanetti, A. Cedeño López, M. d. J. Gálvez-Vázquez, A. Dutta, M. Rahaman and P. Broekmann, *ACS Appl. Mater. Interfaces*, 2018, **10**, 31355-31365.
13. K. Liu, J. Wang, M. Shi, J. Yan and Q. Jiang, *Adv. Energy Mater.*, 2019, **9**, 1900276.
14. K. Jiang, H. Wang, W.-B. Cai and H. Wang, *ACS Nano*, 2017, **11**, 6451-6458.